

# Low-Voltage Distribution Network Impedance Identification Based on Smart Meter Data

Sergey Iakovlev, Robin J. Evans, *Life Fellow, IEEE*, Iven Mareels, *Fellow, IEEE*,

## Abstract

Under conditions of high penetration of renewables, the low-voltage (LV) distribution network needs to be carefully managed. In such a scenario, an accurate real-time low-voltage power network model is an important prerequisite, which opens up the possibility for application of many advanced network control and optimisation methods thus providing improved power flow balancing, reduced maintenance costs, and enhanced reliability and security of a grid.

Smart meters serve as a source of information in LV networks and allow for accurate measurements at almost every node, which makes it advantageous to use data driven methods. In this paper, we formulate a non-linear and non-convex problem, solve it efficiently, and propose a number of fully smart meter data driven methods for line parameters estimation. Our algorithms are fast, recursive in data, scale linearly with the number of nodes, and can be executed in a decentralised manner. The performance of these algorithms is demonstrated for different measurement accuracy scenarios through simulations.

## Index Terms

low-voltage distribution grid, smart meter measurements, impedances identification

## I. INTRODUCTION

The deployment of smart meters at the level of a single customer in the LV power grid opens up the possibility of advanced control and monitoring functions, identification of faults and detection of topology changes. However the most important and developed techniques in state estimation [1], [2], optimal power flow [3], active filtering [4] and economic dispatch all require line impedances and the topology of feeder systems to be known [5], [6]. This information is not always available and when it is available it is often inaccurate. Moreover the increasing emergence of plug-and-play parts in the modern LV distribution grid (e.g. hybrid electric vehicles, renewable generators etc.) further exacerbates this situation. Additionally, certain assumptions for transmission lines in the high voltage (HV) network do not hold for the LV case. For example PMU measurements are a mature technology for HV grids, whereas in LV distribution grids PMU measurements are usually not available primarily due to the high cost [7]. However, the analysis of LV distribution grid estimation in the existing literature often assumes the availability of PMU synchronised measurements [8], [9], [10]. These factors make it difficult to apply the control

S. Iakovlev and R. J. Evans are with the Department of Electrical and Electronic Engineering, The University of Melbourne, Melbourne, VIC 3010, Australia. (e-mail: siakovlev@unimelb.edu.au)

I. Mareels is with IBM Research, Melbourne, VIC 3010, Australia

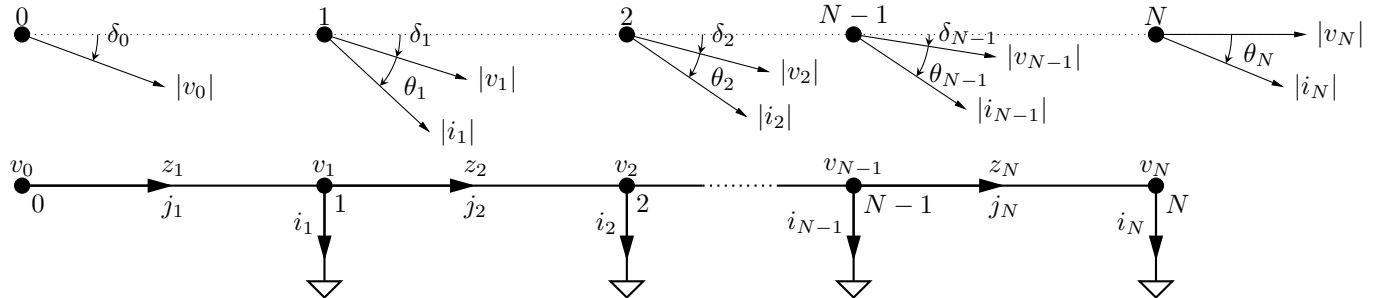


Fig. 1: Bottom: model of a single-phase chain low-voltage distribution feeder. Top: global voltage ( $v_n^g$ ) and current ( $i_n e^{i\delta_n}$ ) phasors at each node. In this figure the phase reference is chosen with respect to the last node  $N$ .

and optimisation methods mentioned above. Hence building a LV grid model based on SM data is an important and potentially valuable opportunity. Smart meters serve as a source of data and provide reliable information about the LV grid which can enable realistic modelling [11].

The most recent research activity is focused on impedance identification methods that allow identification of every single power line impedance ([12], [8]) rather than the grid equivalent impedance as previously [13], [14]. With accurate models these methods open up the possibility for real-time tracking of aging related degradation, faults and electricity theft detection and localisation. Theft is indeed a real issue, e.g. 50% of electricity in developing countries [15], 1-3% (\$6 billion) of total revenue in US [16] and 1% (1200GWh) of electrical energy in Netherlands annually [17]. The most common approach to stealing electricity is a direct connection to the low voltage grid bypassing meter infrastructure completely. Real-time estimation of single power line impedances can help to localise such situations [15].

This paper presents four contributions. First, we propose a recursive approach to low-voltage network modelling based on smart meter data only. Second, we provide a fully decentralised scalable system identification method based on this model and prove its optimality under certain conditions. Third, the method we propose finds a global solution for a class of non-convex optimisation problems in iterative fashion. Fourth, we consider two practical modifications that can improve algorithm performance for industrial applications. Importantly, our algorithms do not require PMU synchronised measurements as is often assumed [7].

The paper is organised as follows. Section II introduces a recursive model for the low-voltage power distribution grid, notations, and presents the main assumptions used through the paper. Section III provides a description of the proposed identification approach and introduces the idea of decentralised grid identification. In Section IV, the algorithm is tested via MATLAB simulations on IEEE test feeder data and its applicability and performance are illustrated. Section V concludes the paper. The appendix contains proofs of certain theoretical results that are used in the paper.

## II. MODEL FORMULATION

In this section we review a circuit theory approach for low voltage power network analysis by considering a chain feeder first and then generalise the results for a tree network.

### A. Notation and preliminaries

The following conventions are used for description of a low-voltage network:

- Node 0 represents a substation transformer.
- Chain feeder nodes and lines are indexed such that  $n$ -th power line connects nodes  $n - 1$  and  $n$ , we denote it as  $(n - 1, n)$ . Therefore all chain feeder parameters have one index.
- A radial power network is represented by a tree graph  $G(\mathcal{N}, \mathcal{E})$  where each node in  $\mathcal{N}$  denotes a bus number and each link  $(k, n) \in \mathcal{E}$  denotes a power line between nodes  $k$  and  $n$ . Power line related parameters in the radial network require two indices.
- Small Latin letters are used for complex or real scalars, i.e.  $a_n = |a_n|e^{i\angle a_n}$  where  $|a_n|$  - amplitude of the complex scalar  $a_n$  and  $\angle a_n$  - its angle. Bold letters are used for vectors ( $\mathbf{a}_n = [a_{1,n}, \dots, a_{M,n}]^T = [a_{1:M,n}]^T$ ) and bold capital letters for matrices ( $\mathbf{A}_n = [a_{1:M,1:N}] = [\mathbf{a}_{1:N}]$ ).

We limit our study to steady state behaviour of a single phase LV grid, when all voltages and currents can be represented as phasors.

### B. Chain feeder Models

Consider a single phase model of a chain low-voltage distribution feeder (Fig. 1) where  $N$  buses (nodes  $1, \dots, N$ ) are connected in series to a distribution transformer (node 0). Every bus  $n$  has voltage  $v_n$  and current  $i_n$ , that are represented as phasors with angle  $\theta_n$  between them. When  $\theta_n > 0$ , current is lagging the voltage. Power line impedances and corresponding line currents are denoted by  $z_n$  and  $j_n$  respectively. By  $\delta_n$  we denote the phase of a voltage phasor with respect to a global reference, for example in Figure 1 the phase reference is chosen with respect to the last node  $N$ .

Throughout this paper we distinguish between global variables, i.e. variables defined with respect to a global phase reference, and local variables, i.e. variables that do not contain global phase angle ( $\delta_n$ ) information:

- $v_n := |v_n|$  - local voltage at the node  $n$ ;
- $v_n^g := |v_n|e^{i\delta_n}$  - global voltage at the node  $n$ ;
- $i_n := |i_n|e^{i\theta_n}$  - local current (consumed or injected) at the node  $n$ ;
- $i_n^g := |i_n|e^{i(\theta_n+\delta_n)} = i_n e^{i\delta_n}$  - global current (consumed or injected) at the node  $n$ ;

Given only local information  $v_n, i_n, \theta_n, z_n$  for all nodes  $n$ , we can calculate unknown node phases  $\delta_n$  and line currents  $j_n$  using Propositions 1 and 2.

**Proposition 1** (Backward model). *Refer to Fig. 1. Let the phase reference be chosen with respect to the last node  $N$  (as in Fig. 1), i.e.  $\delta_N = 0$ . Also, let  $j_n := |j_n|e^{i\beta_n}$  is a local line current, then*

$$\begin{aligned} v_{n-1}e^{i\Delta_n} - v_n &= j_n z_n, \\ j_{n-1} &= i_{n-1} + j_n e^{-i\Delta_n} \end{aligned} \quad (1)$$

for all  $n$ , where  $\Delta_n = \delta_{n-1} - \delta_n$  is the phase increment corresponding to the power line  $(n-1, n)$ .

*Proof.* Define a global line current, flowing between nodes  $n-1$  and  $n$  as  $j_n^g := j_n e^{i\delta_n} = |j_n|e^{i(\beta_n + \delta_n)}$ , i.e. its phase is calculated with respect to the (receiving) node  $n$ , which gives  $j_N^g = i_N$ . Using Ohm's law, we can find the  $(N-1)$ -th node's phase  $\delta_{N-1}$ :

$$v_{N-1}e^{i\delta_{N-1}} - v_N = j_N^g z_N,$$

and from Kirchoff's current law we calculate current  $j_{N-1}^g = i_{N-1}^g + j_N^g$  flowing between nodes  $N-1$  and  $N$ . We repeat this procedure for nodes  $N-2, N-3, \dots, 0$ , find all phases and obtain the following recursive relations for phases and line currents in the feeder:

$$\begin{aligned} v_{n-1}e^{i\delta_{n-1}} - v_n e^{i\delta_n} &= j_n^g z_n, \\ j_{n-1}^g &= i_{n-1}^g + j_n^g. \end{aligned}$$

Divide the first equation by  $e^{i\delta_n}$ , the second by  $e^{i\delta_{n-1}}$ , and then noting that  $j_n^g e^{-i\delta_n} = j_n$ , we obtain the model (1) written in terms of phase increments and local variables.  $\square$

It is often convenient to choose the phase reference with respect to the distribution transformer which leads to the alternative model.

**Proposition 2** (Forward model). *Refer to Fig. 1. Let the phase reference be chosen with respect to the first node in the network, i.e.  $\delta_0 = 0$ . Also, let  $j_n := |j_n|e^{i\phi_n}$  is a local line current, then*

$$\begin{aligned} v_{n-1} - v_n e^{-i\Delta_n} &= j_n z_n, \\ j_{n+1} &= j_n e^{i\Delta_n} - i_n \end{aligned} \quad (2)$$

for all  $n$ , where  $\Delta_n = \delta_{n-1} - \delta_n$  is the phase increment corresponding to the power line  $(n-1, n)$ .

*Proof.* Define a global line current as  $j_n^g := j_n e^{i\delta_{n-1}} = |j_n|e^{i(\phi_n + \delta_{n-1})}$ , i.e. its phase is defined with respect to the (sending) node  $n-1$ . This definition enables us to start consideration from the first node of the chain feeder, where  $\delta_0 = 0$ . Following the same procedure as in the proof of Proposition 1 we obtain:

$$\begin{aligned} v_{n-1}e^{i\delta_{n-1}} - v_n e^{i\delta_n} &= j_n^g z_n, \\ j_{n+1}^g &= j_n^g - i_n^g. \end{aligned}$$

Divide the first equation by  $\delta_{n-1}$  and the second one by  $\delta_n$  we get a model (2) written in terms of phase increments and local variables.  $\square$

*Remark.*

- The forward model has some limitations. For instance, it requires knowledge of the substation transformer current (i.e.  $j_1$  on fig. 1). In the context of impedance identification this means that its magnitude and phase should be known from measurements. However, this is not always the case for LV distribution grids. Another limitation will become apparent when considering the tree network case.
- The forward and backward models are essentially equivalent in that the forward model (2) can be obtained from (1) by multiplying the first equation by  $e^{-i\Delta_n}$  and noting the difference in phases for line current definitions.

### C. Tree network

The results of the previous subsection can be extended to the case of a tree topology. We start from a simple branching example, show how to resolve it using the system of equations (1) and then generalise this approach for any tree network.

**Proposition 3.** *The backward model (1) resolves any network with a tree topology.*

*Proof (Outline).* Consider the network topology case depicted on Fig. 2 which consists of three buses connected in the form of the simplest branching.

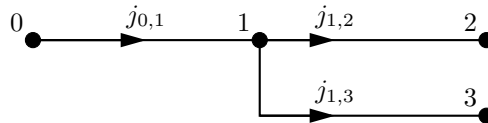


Fig. 2: The simplest branching case

Apply backward model (1) to branches (1,3) and (1,2) simultaneously and find  $\Delta_{1,3}$ ,  $\Delta_{1,2}$ ,  $j_{0,1}$ :

$$\begin{aligned} v_1 e^{i\Delta_{1,3}} - v_3 &= j_{1,3} z_{1,3}, \\ v_1 e^{i\Delta_{1,2}} - v_2 &= j_{1,2} z_{1,2}, \end{aligned} \tag{3}$$

where  $j_{1,3} = i_3$  and  $j_{1,2} = i_2$ . Then

$$j_{0,1} = j_{0,1}^g e^{-i\delta_1} = j_{1,3} e^{-i\Delta_{1,3}} + j_{1,2} e^{-i\Delta_{1,2}} + i_1.$$

Next, we choose the global phase reference and find absolute values of phases at every point in the network. Without loss of generality we can pick  $\delta_2 = 0$ , which gives  $\delta_1 = \Delta_{1,2}$ . Therefore, using the definition of the phase increment introduced earlier,  $\delta = [\delta_0, \delta_1, \delta_3]^T$  can be found from the following system of chain equations:

$$\begin{bmatrix} \Delta_{0,1} \\ \Delta_{1,2} \\ \Delta_{1,3} \end{bmatrix} = \begin{bmatrix} 1 & -1 & 0 \\ 0 & 1 & 0 \\ 0 & 1 & -1 \end{bmatrix} \begin{bmatrix} \delta_0 \\ \delta_1 \\ \delta_3 \end{bmatrix}.$$

The same calculation can be immediately generalised to the case when node 1 has  $n > 2$  links:

$$\begin{bmatrix} \Delta_{0,1} \\ \Delta_{1,2} \\ \vdots \\ \Delta_{1,n-1} \\ \Delta_{1,n} \end{bmatrix} = \begin{bmatrix} 1 & -1 & 0 & \dots & 0 & 0 \\ 0 & 1 & -1 & \dots & 0 & 0 \\ \vdots & \vdots & \vdots & \ddots & \vdots & \vdots \\ 0 & 1 & 0 & \dots & -1 & 0 \\ 0 & 1 & 0 & \dots & 0 & -1 \end{bmatrix} \begin{bmatrix} \delta_0 \\ \delta_1 \\ \vdots \\ \delta_{n-1} \\ \delta_n \end{bmatrix}.$$

It is known from graph theory, that for any tree graph the number of vertices is equal to the number of branches minus one [18, Corollary 1.5.3], i.e. for any tree graph  $G(\mathcal{N}, \mathcal{E})$  with number of nodes/vertices  $|\mathcal{N}|$  and number of branches  $|\mathcal{E}|$ ,  $|\mathcal{N}| = |\mathcal{E}| - 1$ . Thus any tree can be iteratively constructed by adding a pair consisting of a vertex and branch, which shows that the above procedure works for a chain feeder as well as for branching with  $n$  links, therefore it is applicable for any tree network.  $\square$

*Remark.*

- The phase matching procedure is required at branching nodes in a tree topology case, as briefly described in the proof above. For the complete algorithm refer to Algorithm 2 in Section III.
- The forward model (2) is more cumbersome in a branching case. There are additional unknowns that need to be carried until termination. As an example, for the branching on Figure 2:

$$j_{0,1}^g = i_1 e^{i\Delta_{0,1}} + j_{1,2}^g + j_{1,3}^g,$$

currents  $j_{1,2}^g$  and  $j_{1,3}^g$  are unknown, i.e. there are 2 equations, 4 unknowns.

#### D. Discussion

As we saw in the previous sections, the forward model is not well suited to a complete low-voltage network description, hence we use the backward model further in the remainder of this paper.

To conclude the modelling part we present an iterative model directly based on the backward model (1) for a single phase low-voltage network that we will exploit for impedance identification purposes. For any node  $n$ , the set of its ancestors ( $\mathcal{A}_n$ ) and children ( $\mathcal{C}_n$ ) in  $G(\mathcal{N}, \mathcal{E})$  obey an iterative relationship:

$$\begin{aligned} v_n e^{i\Delta_{n,l}} - v_l &= j_{n,l} z_{n,l}, \quad l \in \mathcal{C}_n, \\ \sum_{k \in \mathcal{A}_n} j_{k,n} &= i_n + \sum_{l \in \mathcal{C}_n} j_{n,l} e^{-i\Delta_{n,l}}. \end{aligned} \tag{4}$$

Finally, it is worth noting that the system of equations (4) is not a new model for power networks.

**Proposition 4.** *The system of equations (4) implies the standard power flow model:*

$$\begin{aligned} v_n^2 &= v_l^2 + S_{n,l} z_{n,l}^* + S_{n,l}^* z_{n,l} + |j_{n,l}^g z_{n,l}|^2, \quad l \in \mathcal{C}_n, \\ \sum_{k \in \mathcal{A}_n} S_{k,n} - \sum_{l \in \mathcal{C}_n} (S_{n,l} + |j_{n,l}^g|^2 z_{n,l}) - s_n &= 0. \end{aligned} \tag{5}$$

where  $S_{n,l} = j_{n,l}^{g*} v_l^g$  and  $s_n = i_n^{g*} v_n^g$ .

*Proof.* Exclude the phase term  $e^{i\Delta_{n,l}}$  in (4) and introduce the *receiving-end*<sup>1</sup> complex power flow from  $n$  to  $l$  as  $S_{n,l} = j_{n,l}^{g*} v_l^g = j_{n,l}^* |v_l|$  (since  $j_{n,l}^{g*} v_l^g = j_{n,l}^* e^{-i\delta_l} |v_l| e^{i\delta_l} = j_{n,l}^* |v_l|$ ), and complex power injection  $s_n$  to obtain:

$$v_n e^{i\Delta_{n,i}} - v_i = j_{n,i} z_{n,i}, \quad i \in \mathcal{C}_n,$$

$$\sum_{k \in \mathcal{A}_n} S_{k,n}^* = s_n + \sum_{i \in \mathcal{C}_n} (S_{n,i}^* + |j_{n,i}|^2 z_{n,i}^*).$$

Next, transfer the  $v_i$  term to the right-hand side, take the magnitude squared of the first equation (also, note that  $|j_{n,i}|^2 = |j_{n,i}^g|^2$ ) and complex conjugate of the second equation to obtain the well known power flow model (5).  $\square$

*Remark.* Comparing equations (5) and (4), we notice that the impedance term in the power flow model appears as  $z_{n,l}$  and  $|z_{n,l}|^2$ , whereas the backward model has only  $z_{n,l}$ . Therefore, (4) is a better conditioned set of equations and we prefer it over (5) for the problem of impedance identification, that we consider in detail in the next section.

### III. SYSTEM IDENTIFICATION

In this section we consider the problem of system identification, that is, the problem of identifying impedances in a low-voltage network and we develop an approach that exploits the iterative structure of the backward model (4). We work through the details for a chain feeder model, however the proposed method can be generalised to any tree network as described earlier. We first formulate the optimisation problem for the whole network and then consider two methods to solve it approximately.

We start by considering the same chain feeder model as before (fig. 1) with the following measurements available:

- $v_0$  - RMS<sup>2</sup> substation transformer voltage,
- $\mathbf{v}_n = [v_n^{(1)}, \dots, v_n^{(M)}]^T$  - RMS voltage measurements at node  $n$ ,
- $|\mathbf{i}_n| = [|\mathbf{i}_n^{(1)}|, \dots, |\mathbf{i}_n^{(M)}|]^T$  - RMS consumption current measurements at node  $n$ ,
- $\boldsymbol{\theta}_n = [\theta_n^{(1)}, \dots, \theta_n^{(M)}]^T$  - angle measurements between voltage and current phasors,

where indices  $n = 1 : N$  and  $m = 1 : M$  are used for node and measurement number respectively, e.g.  $v_n^{(m)}$  - RMS value of the voltage at node  $n$  corresponding to the  $m$ -th measurement<sup>3</sup>. According to the minimum functionality requirements for smart metering infrastructure in Australia, every smart meter should be capable of measuring total active power, reactive power and voltage magnitude [19, Table 6 – 2], which is equivalent to availability of  $\mathbf{v}_n, |\mathbf{i}_n|, \boldsymbol{\theta}_n$  for all  $n$ .

Regarding the measurements we assume the following.

**Assumption 1.** Smart meter measurements can be considered time synchronised with respect to system changes, i.e. for the  $m$ -th measurement taken from every node in the network, load impedances remain constant. This is justified because smart metering minimum functionality specifications require smart meters to maintain measurement time clocks to within a few seconds across a network, see e.g. [19, Chapter 7.5],[20, Chapter 6].

<sup>1</sup>Note that the sign for terms with  $|j_{n,l}|^2$  in resulting power flow equations is reversed with respect to the case when branch power is defined as sending-end complex power flow, i.e.  $S_{n,l} = j_{n,l}^* v_n$ .

<sup>2</sup>Root mean square

<sup>3</sup>Although the index  $m$  is used for measurement number, it does not necessarily mean that the corresponding quantity is measured, e.g. the value of  $j_n^{(m)}$  corresponds to  $m$ -th measurement, but it is not measured directly and must be derived from other measurements.

*Remark.* Note that when PMU is available  $v_n^g$  and  $i_n^g$  values are measured directly. In contrast, the smart meter measurements  $(v_n, |i_n|)$  do not contain global phases  $\delta_n$ . Nevertheless, the phase synchronism provided by PMU is not needed for our algorithms.

**Assumption 2** Line impedances and grid topology remain unchanged during the whole measurement process.

*Remark.* Algorithms that we develop in the next section allow us to monitor varying line impedances and, therefore, detect topology changes.

**Assumption 3.** Smart meter measurement uncertainty is approximated by Gaussian noise  $\mathcal{N}(0, \sigma)$ , where  $\sigma$  corresponds to 1% full scale<sup>4</sup> error which is practical for the majority of household smart meters, see e.g. technical reports [20, Chapter 4], [19, Chapter 7.1].

*Remark.* Note, however, that 1% of full scale error for voltage, current and angle corresponds to about 2% error in measured power, i.e. this setup can be considered as a worst case. Thus, we also consider 0.5% and 0.1% of full scale error cases.

#### A. Problem formulation. Chain feeder

Consider a chain feeder (Fig. 1) and formulate the problem of identifying impedances based on the backward model (1) written in multidimensional form (i.e. when multiple measurements are gathered):

$$\begin{aligned} \mathbf{v}_{n-1}e^{i\Delta_n} - \mathbf{v}_n &= \mathbf{j}_n z_n, \\ \mathbf{j}_{n-1} &= \mathbf{i}_{n-1} + \mathbf{j}_n e^{-i\Delta_n}, \end{aligned} \quad (6)$$

where  $\mathbf{v}_n = [v_n^{(1)}, \dots, v_n^{(M)}]^T$ ,  $\mathbf{j}_n = [j_n^{(1)}, \dots, j_n^{(M)}]^T$ ,  $\Delta_n = [\Delta_n^{(1)}, \dots, \Delta_n^{(M)}]^T$  and  $e^{i\Delta_n}$  is a component-wise operation as well as multiplication of two vectors  $\mathbf{v}_{n-1}e^{i\Delta_n}$  and  $\mathbf{j}_n e^{i\Delta_n}$ .

Next, define a cost function for the  $n$ -th power line based on the first equation in (6):

$$c_n(z_n, \mathbf{j}_n, \Delta_n) = \left\| \mathbf{v}_{n-1}e^{i\Delta_n} - \mathbf{v}_n - \mathbf{j}_n z_n \right\|_2^2, \quad (7)$$

and introduce a cost-to-go function

$$J_{k:N} = \sum_{n=k}^N c_n(z_n, \mathbf{j}_n, \Delta_n) \quad (8)$$

for lines  $N, N-1, \dots, k$ . Using the second equation in (6) we formulate the problem of impedance identification in a chain feeder:

$$\begin{aligned} &\text{minimise}_{z_{1:N}, \Delta_{0:N-1}} J_{1:N} \\ &\text{subject to} \quad \mathbf{j}_{n-1} = \mathbf{i}_{n-1} + \mathbf{j}_n e^{-i\Delta_n}, \\ &\quad \quad \quad \mathbf{j}_N = \mathbf{i}_N, \\ &\quad \quad \quad n = 1, \dots, N-1. \end{aligned} \quad (9)$$

The main advantage of this formulation is that the computation complexity scales linearly with the number of nodes, although the resulting optimisation problem is non-linear and non-convex. In the next subsections we consider two simplifications that allow solution for different practical scenarios.

<sup>4</sup>i.e. the error value is taken with respect to the full scale of the measurement device



### B. Identification algorithm. Linearised case

The first simplification is based on the following assumption which is very common in the analysis of low-voltage grids [21].

**Assumption 4** The phase increments  $\Delta_n$  are negligibly small.

*Remark.* Note, that we neglect the phase increments but we do not neglect the absolute phase at each node in the network.

Under Assumption 3, the model (6) takes the form:

$$\begin{aligned} \mathbf{v}_{n-1} - \mathbf{v}_n &= \mathbf{j}_n z_n, \\ \mathbf{j}_{n-1} &= \mathbf{i}_{n-1} + \mathbf{j}_n. \end{aligned} \tag{10}$$

Then the cost function (7) can be linearised and rewritten as follows by splitting it into real and imaginary parts:

$$c_n^l(\mathbf{z}_n, \mathbf{j}_n) = \left\| \mathbf{v}_{n-1} - \mathbf{v}_n - \mathbf{J}_n \mathbf{Q}_1 \mathbf{z}_n \right\|_2^2 + \left\| \mathbf{J}_n \mathbf{Q}_2 \mathbf{z}_n \right\|_2^2, \tag{11}$$

where  $\mathbf{J}_n := [\text{Re } \mathbf{j}_n \quad \text{Im } \mathbf{j}_n]$ ,  $\mathbf{z}_n := [\text{Re } z_n \quad \text{Im } z_n]^T$ ,  $\mathbf{Q}_1 := \begin{bmatrix} 1 & 0 \\ 0 & -1 \end{bmatrix}$  and  $\mathbf{Q}_2 := \begin{bmatrix} 0 & 1 \\ 1 & 0 \end{bmatrix}$ . Therefore, we obtain the optimisation problem of the form:

$$\begin{aligned} &\text{minimise}_{\mathbf{z}_{1:N}} J_{1:N}^l \\ &\text{subject to} \quad \mathbf{j}_{n-1} = \mathbf{i}_{n-1} + \mathbf{j}_n, \\ &\quad \mathbf{j}_N = \mathbf{i}_N, \\ &\quad n = 1, \dots, N-1. \end{aligned} \tag{12}$$

where  $J_{1:N}^l = \sum_{n=1}^N c_n^l(\mathbf{z}_n, \mathbf{j}_n)$  is the corresponding linearised cost-to-go function.

This problem can be approached from the dynamic programming perspective. To show this, consider the cost-to-go function for the last two power lines:

$$\begin{aligned} J_{N-1:N} &= \min_{\mathbf{z}_{N-1:N}} [c_{N-1}^l(\mathbf{z}_{N-1}, \mathbf{j}_{N-1}) + c_N^l(\mathbf{z}_N, \mathbf{j}_N)] = \\ &= \min_{\mathbf{z}_{N-1}} [c_{N-1}^l(\mathbf{z}_{N-1}, \mathbf{i}_{N-1} + \mathbf{j}_N)] + \min_{\mathbf{z}_N} [c_N^l(\mathbf{z}_N, \mathbf{j}_N)], \end{aligned}$$

where both terms are the impedance identification problems for lines  $N$  and  $N-1$ . Using the same argument for all power lines in the feeder, we conclude that minimising sum in (9) is equivalent to minimising each term separately according to Algorithm 1. Since it identifies the network starting from the edge node and propagating all the way through to the first node, we call it LBCI (Linearised Backward Calculation of Impedances).

---

**Algorithm 1** LBCI algorithm for a chain feeder
 

---

```

1:  $\mathcal{M} := \{\mathbf{v}_n, |\mathbf{i}_n|, \boldsymbol{\theta}_n \mid n = 1, \dots, N\} \cup \{\mathbf{v}_0\}$ 
2: function LBCI( $\mathcal{M}$ )
3:    $\mathbf{j}_N = \mathbf{i}_N$ 
4:   for  $n = N : 1$  do
5:      $\hat{\mathbf{z}}_n = \operatorname{argmin}_{\mathbf{z}_n} c_n^l(\mathbf{z}_n, \mathbf{j}_n)$ 
6:      $\mathbf{j}_{n-1} = \mathbf{i}_{n-1} + \mathbf{j}_n$ 
7:   return  $\hat{\mathbf{Z}} = [\hat{\mathbf{z}}_{1:N}], \mathbf{J} = [\mathbf{j}_{1:N}]$ 

```

---

*Remark.*

- Minimisation of  $c_n^l(\mathbf{z}_n, \mathbf{j}_n)$  with respect to  $\mathbf{z}_n$  is a simple unconstrained least squares problem, where the second term can be interpreted as a regularisation term. Note, that it appears naturally in the problem formulation.
- Formally, measurement noise affects the  $\mathbf{J}_n$  term, since it contains data (real and imaginary parts of  $\mathbf{j}_n$ ) derived from measurements. In practice, the main source of error is the voltage measurement noise, therefore the error in matrix  $\mathbf{J}_n$  can be neglected in favour of using a linear least squares approach. Linear least squares estimation is also preferable as a simple (from a computational perspective for decentralised implementation) and flexible (i.e. has recursive, weighted modifications) method. This allows real-time tracking of impedances in the network as new measurements become available. Nevertheless, when errors in  $\mathbf{J}_n$  need to be taken into account, total least squares (TLS) techniques can be used [22].
- There is widely used variation of LBCI algorithm where the regularisation part is ignored in (11), i.e.:

$$c_n^l(\mathbf{z}_n, \mathbf{j}_n) = \left\| \mathbf{v}_{n-1} - \mathbf{v}_n - \mathbf{J}_n \mathbf{Q}_1 \mathbf{z}_n \right\|_2^2$$

We refer to this algorithm as LBCI-old. In [23] a very similar approach is used, although the main difference from the case we consider is computation complexity. The authors propose solving a least-squares problem with measurement matrix of size  $MN \times (M + 2N)$  which has complexity around  $O((M + 2N)^2 MN)$  whereas in our case we solve  $N$  problems with  $M \times 2$  matrices which results in  $O(MN)$ .

Generalisation to a tree topology feeder involves one extra step: we need to keep track of phase increments in order to match the absolute phases of line currents at the intersection point. Note, that because of linearisation we do not obtain correct values of absolute phases, however this is not an issue for identification purposes, since the backward model (1) is based on the incremental phase information.

Let  $\mathcal{M}^i$  and  $\mathcal{M}^j$  be the sets of measurements for branches  $i$  and  $j$  that have a common node  $n^*$  and sets of indices  $\mathcal{N}^i$  and  $\mathcal{N}^j$  correspondingly. We briefly summarise the procedure of phase matching:

---

**Algorithm 2** Phase matching procedure
 

---

1: Calculate:

$$\widehat{\mathbf{Z}}^i, \mathbf{J}^i = \text{LBCI}(\mathcal{M}^i), \quad \widehat{\mathbf{Z}}^j, \mathbf{J}^j = \text{LBCI}(\mathcal{M}^j).$$

2: For a common node  $n^*$  find absolute phases as a sum of phase increments  $\Delta_k$ <sup>5</sup>:

$$\Delta_k = \frac{\mathbf{J}_k \mathbf{Q}_2 \widehat{\mathbf{Z}}_k^i}{v_{k-1}}, \quad \delta_{n^*}^i \approx \sum_{k \in \mathcal{N}_i} \Delta_k, \quad \delta_{n^*}^j \approx \sum_{k \in \mathcal{N}_j} \Delta_k.$$

3: Chose  $\delta_{n^*}^i$  as a reference and update phases in branch  $j$  by a factor of  $\delta_{n^*}^i - \delta_{n^*}^j$ . This is shown by black arrows in Fig. 3.

---

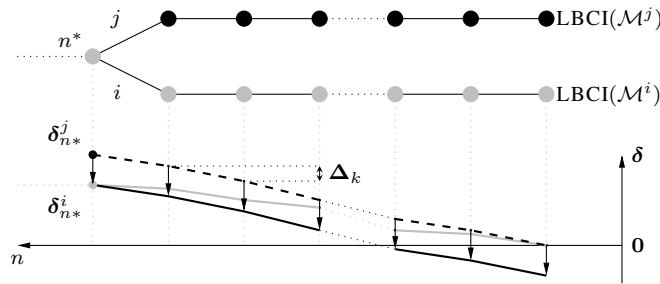


Fig. 3: Phase matching procedure example. Top: two branches  $i$  (grey dots) and  $j$  (black dots). Bottom: corresponding phase plots. The grey line is the phase of the reference branch  $i$ , dotted line shows the initial phase for branch  $j$ , black solid line is the updated phase for branch  $j$ .

The illustration of this procedure is given in Figure 3, where the black dotted line, corresponding to the phases along  $j$ -th branch before matching, gets shifted by the amount of phase difference at the node  $n^*$ . The complete algorithm for a tree topology case can be obtained by combining this procedure with the chain feeder algorithm. Therefore, under the linearisation assumption (Assumption 3), the problem of impedance identification can be solved optimally.

To conclude, the developed algorithm is fast, simple and can be implemented in a distributed fashion, as discussed in Section III-E. However, we lose information about phase angle increments at each power line which leads to unknown absolute phase at each node. It turns out that we can address this issue very efficiently without losing the key properties of the developed algorithm.

### C. Identification algorithm. Non-linear case

In this section we consider an alternative simplification of (9) where minimisation of each cost function (7) is a non-linear and non-convex problem. Noticeably, any such problem has certain properties that can be exploited in order to solve it globally. Although the modification we introduce does not lead to a global solution of the original

<sup>5</sup>Formula for  $\Delta_k$  is obtained from (6) after taking imaginary part of the first equation.

non-linear problem (9), we show that any solution it finds is closer to the global optimum of (9) than that found in linearised case.

Consider the cost function (7) and, using the notation introduced in (11), write it as follows by splitting real and imaginary parts:

$$c_n(\mathbf{z}_n, \mathbf{j}_n, \gamma_n) = \left\| \mathbf{V}_{n-1}\gamma_n - \mathbf{v}_n - \mathbf{J}_n \mathbf{Q}_1 \mathbf{z}_n \right\|_2^2 + \left\| \mathbf{V}_{n-1}\sqrt{\mathbf{1} - \gamma_n^2} - \mathbf{J}_n \mathbf{Q}_2 \mathbf{z}_n \right\|_2^2, \quad (13)$$

where  $\gamma_n := \cos \Delta_n$ ,  $\mathbf{V}_n := \text{diag}(\mathbf{v}_n)$ ,  $\mathbf{1} = [1, \dots, 1]^T$ , operations  $\sqrt{(\cdot)}$ ,  $\cos(\cdot)$  and  $(\cdot)^2$  are component-wise.

Next, instead of minimising the original cost  $c_n(\mathbf{z}_n, \mathbf{j}_n, \gamma_n)$  at each step, we minimise the first term and use the second term as a constraint:

$$\begin{aligned} & \text{minimise}_{\gamma_n, \mathbf{z}_n} \left\| \mathbf{V}_{n-1}\gamma_n - \mathbf{v}_n - \mathbf{J}_n \mathbf{Q}_1 \mathbf{z}_n \right\|_2^2 \\ & \text{subject to} \quad \gamma_n = \sqrt{\mathbf{1} - \frac{(\mathbf{J}_n \mathbf{Q}_2 \mathbf{z}_n)^2}{\mathbf{v}_{n-1}^2}}, \end{aligned} \quad (14)$$

where operations  $\frac{(\cdot)}{(\cdot)}$  and  $(\cdot)^2$  are component-wise. The reasoning behind this formulation will become clear in the next subsection where we make comparison with the LBCI algorithm.

*Remark.* In the constraint equation for  $\gamma_n$  we use only the positive root. By doing so, we restrict consideration for phase angles  $\Delta_n^{(m)} \in [-\pi/2; \pi/2]$  (or  $0 \leq \gamma_n^{(m)} \leq 1$ ) which is practical for low-voltage power networks.

The main idea for the optimisation algorithm is based on Lemma 1 (see Appendix). In the context of problem (14), let:

$$\begin{aligned} f(\gamma_n, \mathbf{z}_n) &:= \left\| \mathbf{V}_{n-1}\gamma_n - \mathbf{v}_n - \mathbf{J}_n \mathbf{Q}_1 \mathbf{z}_n \right\|_2^2, \\ g(\mathbf{z}_n) &:= \sqrt{\mathbf{1} - \frac{(\mathbf{J}_n \mathbf{Q}_2 \mathbf{z}_n)^2}{\mathbf{v}_{n-1}^2}}, \\ h(\gamma_n) &:= [\mathbf{J}_n \mathbf{Q}_1]^\dagger (\mathbf{V}_{n-1}\gamma_n - \mathbf{v}_n). \end{aligned}$$

First, we check if the requirements of Lemma 1 are satisfied:

- $\mathbf{V}_{n-1}$  is a full rank matrix since  $\mathbf{V}_{n-1} = \text{diag}(\mathbf{v}_{n-1})$ . Regarding  $\mathbf{J}_n$ , we assume that it is a full rank matrix, in other words, there should be enough variation in measurements.
- $g(\mathbf{z}_n)$  is a surjective mapping for all  $\mathbf{z}_n$  that satisfy:

$$(\mathbf{J}_n \mathbf{Q}_2 \mathbf{z}_n)^2 \leq \mathbf{v}_{n-1}^2$$

This condition requires that the voltage drop at the line is less than or equal to the voltage at its node, which is always true for low-voltage networks.

*Remark.*  $\mathbf{J}_n$  is not a full rank matrix if it contains identical measurements or if the line current is zero for all measurements except one. Both cases are pathological, and to handle them in practise, we introduce regularisation term into the problem formulation (see the next subsection). There is another case when  $\mathbf{J}_n$  becomes singular: a power factor among all loads in the feeder is the same and remains constant, which is also highly improbable. We address this problem in simulations (see section IV).

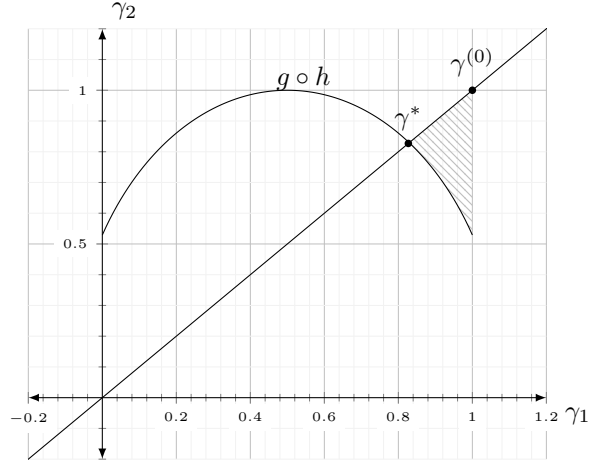


Fig. 4: Area maximisation problem for a scalar case. The objective is to maximise the area between  $g \circ h$  and a line, starting from  $\gamma^{(0)}$ . The result is shown in dashed gray.

Second, according to Lemma 1 we need to find a fixed point of  $g \circ h$ .

**Proposition 5.** *A fixed point of  $g \circ h$  can be found via the following iteration:*

$$\gamma_n^{(i+1)} = \gamma_n^{(i)} + \alpha [g \circ h(\gamma_n^{(i)}) - \gamma_n^{(i)}], \quad \gamma_n^{(0)} = \mathbf{1}, \quad (15)$$

where  $0 < \alpha < 1$ .

*Proof.* The iteration (15) is a gradient descent type algorithm for the area maximisation problem. To see this, consider:

$$\nabla_{\gamma_n} \left[ \int_{\gamma_n^{(0)}}^{\gamma_n} [g \circ h(\bar{\gamma}_n) - \bar{\gamma}_n] d\bar{\gamma}_n \right] = g \circ h(\gamma_n) - \gamma_n.$$

As follows from the properties of definite integrals, the function in brackets is strictly increasing and therefore standard optimisation techniques can be applied in order to find its global maximum. Figure 4 illustrates this idea for some scalar function  $g \circ h$ .

□

*Remark.*

- The sign of  $\alpha$  defines the direction of integration. For instance, in (15) the direction is chosen so, that the iteration converges to the  $\mathbf{0} \leq \gamma_n^* \leq \gamma_n^{(0)}$ . Importantly,  $\gamma_n^*$  that solves (14) is always non-negative, this property allows using iteration (15) and obtain a global solution.
- In the context of power systems, at the first step ( $i = 0$ ) of the iteration (15) we solve the minimisation problem (14) with chain approximation around  $\gamma_n = \mathbf{1}$ . This is equivalent to Assumption 2 (see previous subsection). At the next iteration the algorithm consequently improves previous estimation converging to the solution.

---

**Algorithm 3** Local iteration for a single power line.

---

```

1:  $\mathcal{M}_{n-1:n} := \{\mathbf{v}_k, |\mathbf{i}_k|, \boldsymbol{\theta}_k \mid k = n, n-1\}$ 
2: function LINECALC( $\mathcal{M}_{n-1:n}, \epsilon, \alpha, \mathbf{j}_n$ )
3:    $i = 0, \gamma_n^{(0)} = \mathbf{1}$ 
4:   do
5:      $\hat{\mathbf{z}}_n^{(i)} = \mathbf{h}(\gamma_n^{(i)})$ 
6:      $\gamma_n^{(i+1)} = \gamma_n^{(i)} - \alpha \left[ \mathbf{g}(\hat{\mathbf{z}}_n^{(i)}) - \gamma_n^{(i)} \right]$ 
7:     while  $\|\mathbf{g}(\hat{\mathbf{z}}_n^{(i)}) - \gamma_n^{(i)}\|_2 > \epsilon$ 
8:   return  $\hat{\mathbf{z}}, \gamma$ 

```

---

Finally, we formalise the resulting identification algorithm with iteration (15) for a single power line between nodes  $n-1$  and  $n$  in Algorithm 3. Note, that this algorithm uses information from the previous line of the network, i.e. it needs  $\mathbf{j}_n$  to be known. Therefore, using the backward model (1) iteratively we formulate the complete algorithm for a chain feeder identification in Algorithm 4

---

**Algorithm 4** BCI algorithm for a chain feeder.

---

```

1:  $\mathcal{M} := \{\mathbf{v}_n, |\mathbf{i}_n|, \boldsymbol{\theta}_n \mid n = 1, \dots, N\} \cup \{\mathbf{v}_0\}$ 
2: function BCI( $\mathcal{M}, \epsilon, \alpha$ )
3:    $\mathbf{j}_N = \mathbf{i}_N$ 
4:   for  $n = N : 1$  do
5:      $\hat{\mathbf{z}}_n, \gamma_n = \text{LINECALC}(\mathcal{M}_{n-1:n}, \epsilon, \alpha, \mathbf{j}_n)$ 
6:      $\mathbf{j}_{n-1} = \mathbf{i}_{n-1} + \mathbf{j}_n \frac{|v_n|}{|v_{n-1}|} + \hat{\mathbf{z}}_n^* \frac{|\mathbf{j}_n|^2}{|v_{n-1}|}$  ▷ (*)
7:   return  $\gamma, \hat{\mathbf{z}}, \mathbf{j}$ 

```

---

*Remark.* Equation (\*) in the Algorithm 4 can be obtained from the backward model (1) after excluding term  $e^{i\Delta_n}$ .

#### D. Discussion

The main objective of impedance identification algorithm is to minimise a cost function given by (13) for each power line. In this section we compare the optimality of solutions found by BCI and LBCI algorithms.

Again, consider a power line connecting nodes  $n-1$  and  $n$ . The following proposition holds for solutions found by LBCI and BCI:

**Proposition 6.** *Let  $(\mathbf{z}_n^{LBCI}, \mathbf{1})$  is the solution found by the LBCI algorithm and  $(\mathbf{z}_n^{BCI}, \gamma_n^{BCI})$  is the solution found by the BCI algorithm. Also, let  $N(\mathbf{z}_n, \gamma_n) := \|\mathbf{V}_{n-1}\gamma_n - \mathbf{v}_n - \mathbf{J}_n \mathbf{Q}_1 \mathbf{z}_n\|_2^2 + \|\mathbf{V}_{n-1}\sqrt{\mathbf{1} - \gamma_n^2} - \mathbf{J}_n \mathbf{Q}_2 \mathbf{z}_n\|_2^2$  then*

$$N(\mathbf{z}_n^{BCI}, \gamma_n^{BCI}) \leq N(\mathbf{z}_n^{LBCI}, \mathbf{1}),$$

*i.e. the BCI algorithm finds the solution that is closer to the optimum of (9) than that of LBCI.*

*Proof.* See appendix. □

*Corollary.* In the presence of high measurement noise, we can introduce a regularisation term (as in the LBCI case) for BCI algorithm so that:  $N(\mathbf{z}_n^{BCI}, \gamma_n^{BCI}) \leq N(\mathbf{z}_n^{LBCI}, \mathbf{1})$ .

*Proof.* See appendix. □

Importantly, all the key properties of the LBCI algorithm are inherited by the BCI algorithm, since  $\mathbf{h}(\gamma_n^{(i)})$  is a least squares solution of the unconstrained problem (14) for a given  $\gamma_n^{(i)}$ .

### E. Practical modifications

This subsection describes some additional modifications that improve the LBCI/BCI algorithm performance.

We start from the idea of decentralised calculations, whereby the BCI algorithm above can be executed by smart meters in a decentralised manner with a modification to take advantage of a known  $X/R$  ratio<sup>6</sup> from cable data.

**Regularisation.** As was mentioned in the section III-C, if elements in  $\mathbf{J}_n$  are equal to zero (or close to it) then  $\mathbf{J}_n$  is no longer a full rank. To address this issue we can add regularisation term to the objective function in (14), i.e:

$$\left\| \mathbf{V}_{n-1}\gamma_n - \mathbf{v}_n - \mathbf{J}_n \mathbf{Q}_1 \mathbf{z}_n \right\|_2^2 + \mu \|\mathbf{D} \mathbf{z}_n\|_2^2,$$

where  $0 \leq \mu \leq 1$ ,  $\mathbf{D} = \mathbf{J}_n \mathbf{Q}_2$  as was discussed in the previous subsection. However, note that the choice of  $\mathbf{D}$  and  $\mu$  depends on a priori knowledge about power lines in the network. Thus an algorithm designer might want to incorporate information, that  $X/R$  ratio for a cable is close to 1, by making  $\mathbf{D} = [1 \ -1]$ .

**X/R modification.** One method to improve algorithm performance with respect to noise is to use reactance-to-resistance ratio ( $k_n$  for  $n$ -th power line) usually available from cable specifications. The matrix  $\mathbf{J}_n$  (first defined in (11)) with  $X/R$  modification becomes a vector of size  $M$  by 1, therefore its condition number  $\kappa(\mathbf{J}_n) = 1$ , which leads to a better noise resistivity for impedance estimation:

$$\mathbf{J}_n = \text{Re}(\mathbf{j}_n) - k_n \text{Im}(\mathbf{j}_n).$$

Whenever the algorithm has information about  $X/R$  ratio of a cable we add subscript  $(\cdot)_{XR}$  to its name, i.e.  $\text{BCI}_{XR}$  or  $\text{LBCI}_{XR}$ .

**Decentralisation.** The LBCI/BCI algorithm estimates power line impedances for all nodes by processing them sequentially. Thus, for large scale networks large memory required in order to store information from all smart meters. However, every iteration uses data only from neighbouring nodes, therefore one iteration can be encapsulated within one smart metering device capable of obtaining data from adjacent nodes, i.e. from neighbouring smart meters. This makes the grid estimation procedure secure and scalable.

Consider the case of the BCI algorithm and suppose that every smart meter can communicate with its immediate neighbours and the smart meter at node  $n+1$  has already calculated values of  $\mathbf{j}_{n+1}$  as in Fig. 5. Then it sends data to the adjacent smart meter at the  $n$ -th node, which now has enough information to calculate the impedance of the

<sup>6</sup> $X/R$  ratio is the ratio between inductance and resistance of the cable

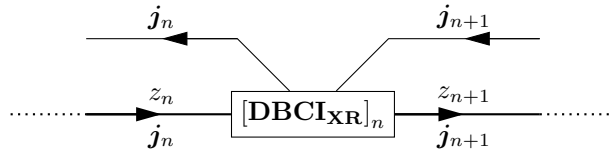


Fig. 5: Smart meter at  $n$ -th node. Concept of decentralised BCI with known  $X/R$  ratio

power line connecting these two meters by performing several iterations of the original BCI algorithm. In addition, it calculates the input current  $\mathbf{j}_n$  and sends it further up the feeder to the next smart meter and so on. Furthermore, this approach allows each device to have its own information about the  $X/R$  ratio for the power lines to which it is connected. The resulting algorithm is called Decentralised BCI with  $X/R$  modification, i.e.  $\text{DBCI}_{XR}$ .

#### IV. NUMERICAL SIMULATIONS

In order to test the algorithms a single phase power network chain feeder as in Fig. 1 was implemented in MATLAB/Simulink with  $N = 10$ . Each power line is modelled as a series connection of resistance and inductance, which is realistic for low voltage overhead lines up to 1-2 km in length [24]. Loads are modelled as a parallel connection of resistance, inductance and capacitance. Their load shapes are taken from IEEE Low Voltage European Test Feeder data with minute resolution measurements. Although some domestic loads consist of a very complicated composition of resistive, inductive and non-linear parts [25], [26] we limit our simulations as described above, since our algorithm has full information about load impedances via smart meter measurements. We conduct 5000 measurements for all tests, which is equivalent to around 4 days of a network operation.

To illustrate important features of algorithms developed in the paper we consider two separate cases:

- No measurement noise. All lines are of the same lengths (50m and 500m).
- With measurement noise added (1%, 0.5% and 0.1%). All lines are of the same lengths (50m and 500m).

Long lines are chosen in order to show the important properties of the BCI algorithm.

##### A. LBCI/BCI testing under ideal conditions

We first show BCI performance under ideal conditions, when measuring devices do not have measurement error. To demonstrate the main features of a proposed algorithm we use oversimplified conditions. Each line has the following parameters: length - 50m,  $R = 0.4 \Omega/km$ ,  $X/R$  ratio - 0.7. According to IEEE Low Voltage European Test Feeder data description the power factor is kept constant for each load. This is a good assumption for a high level analysis, however, for our algorithms the more detailed behaviour is required. To model uncertainty in power factor we vary it between 0.9 and 1 as a random Gaussian variable ( $\mu = 0.95, \sigma = 0.05$ ) for each load.

We first show algorithm performance with known  $X/R$  ratio, since in this case, the result does not depend on the condition number of the measurement matrix ( $\mathbf{J}_n$ ). Figure 6 (left) illustrates identification relative error of BCI algorithm after different number of iterations. The red dotted line on the figure corresponds to the linearised case, i.e. when we assume a small phase difference ( $\Delta_n \ll 1$ ) between two nodes. Note, that it coincides with a very



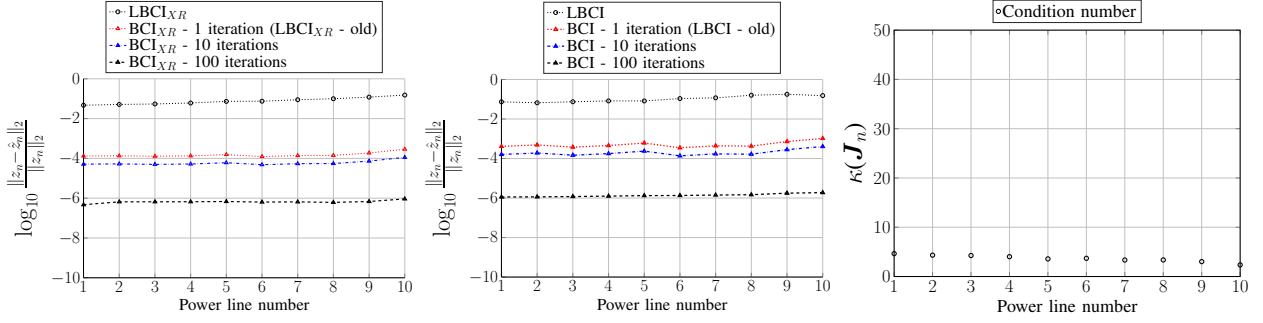


Fig. 6: Impedance identification error for each power line. FBCI and BCI algorithms under ideal conditions (left, centre). Condition number for matrix  $J_n$  (right).

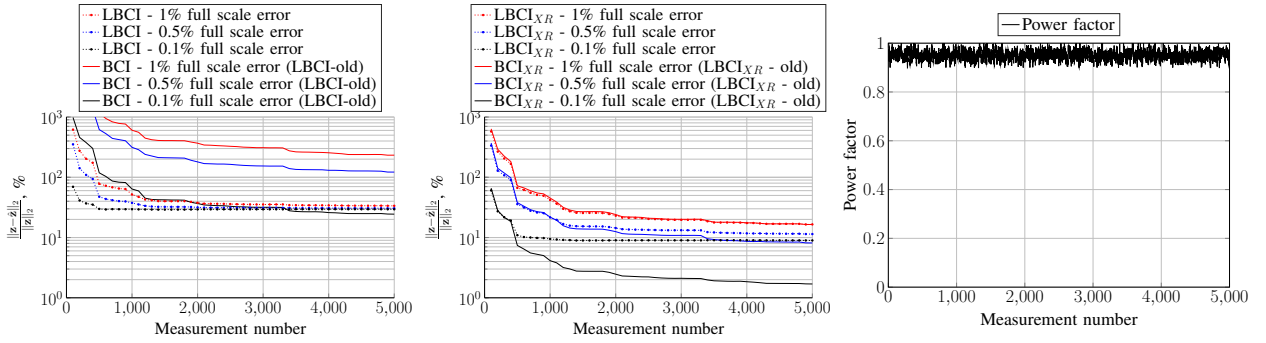


Fig. 7: Dependence of impedance identification error on measurement number. BCI algorithm under noisy conditions. Averaged over 100 realisations.

common in the literature LBCI approach. Blue, and black lines show the relative error after 10 and 100 iterations correspondingly. The step size  $\alpha$  was chosen to be 0.1. After about 30 iterations the error is close to simulation accuracy. Note that the same result is unachievable with LBCI or LBCI-old algorithms.

The next figure (Fig. 6 - centre) compares BCI algorithm performance under ideal conditions with LBCI. Note, that the corresponding line current matrix  $J_n$  has a condition number around 4-5 for a given set of load shapes from LV European Test Feeder data (Fig. 6 - right) and with power factor disturbances introduced. Thus the performance of algorithms is slightly worse than in the previous case, however the result of BCI algorithm is still very close to the simulation accuracy limit. Again, LBCI-old coincides with the first iteration of the BCI algorithm.

### B. LBCI/BCI testing with modifications under noisy conditions

In this subsection we introduce Gaussian noise to model different accuracy classes (1%FS, 0.5%FS and 0.1%FS) of commercially available smart meters and test FBCI and BCI algorithms performance under these conditions. Usually, accuracy class is specified as a percentage of a full scale with 95% confidence interval (i.e. two standard deviations in our case). Again, we conduct two tests: when  $X/R$  ratio is given and without it. In addition we consider a scenario when power factor variations are much larger, i.e. Fig 8 (right) as an example for such variations for a particular load.

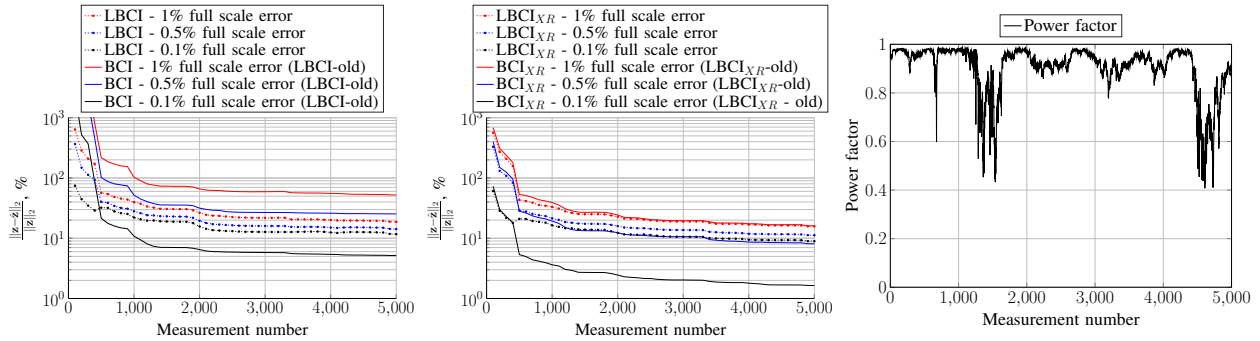


Fig. 8: Dependence of impedance identification error on measurement number. BCI algorithm under noisy conditions. Averaged over 100 realisations.

Figure 7 shows the identification error dependence on the measurements number for three accuracy classes listed above using LBCI and BCI algorithms. In Figure 7 (left) the results are shown when  $X/R$  ratio is unknown a priori. In this case LBCI outperform both BCI and conventional LBCI-old algorithms, providing more accurate identification as well as significantly smaller amount of computations. However, note how BCI algorithm outperforms LBCI in the Figure 7 (right), i.e. when condition number of  $\kappa(\mathbf{J}_n) = 1$ . This shows that when the condition number of matrix  $\mathbf{J}_n$  decreases, the quality of BCI estimation significantly increases. The same applies to LBCI-old algorithm, its estimation results almost coincide with BCI ones. To demonstrate the effect of condition number of  $\mathbf{J}_n$ , we conducted an additional simulation, using the same feeder, but with much higher power factor variations (see Figure 8). Note, how BCI algorithm outperforms LBCI for measurements with 0.1% accuracy by a factor of 4 when  $XR$  ratio is unknown, and by a factor of 5 when it is known, almost achieving 1% of impedances estimation accuracy.

*Remark.* Although, LBCI algorithm shows better results for 1% and 0.5% measurement accuracy cases there are two key properties should be mentioned:

- The gap between BCI and LBCI performance curves for different power factor variation scenarios is reduced by a factor of 5 and 3 respectively, which shows that BCI algorithms outperforms LBCI provided enough variation in the grid.
- BCI performance can achieve the same (even slightly better according to corollary for Proposition 6) level of accuracy by adding a regularisation term.

### C. BCI testing with long power lines

The previous tests under noisy condition did not show the main advantage of using BCI over LBCI-old and, in some cases, LBCI algorithms. However, it can be observed when using long lines in the network, which happens quite often in sparsely populated places. The same simulation was conducted with the lines 500m each with unknown  $X/R$  ratios. The results are shown in the Figure 9.

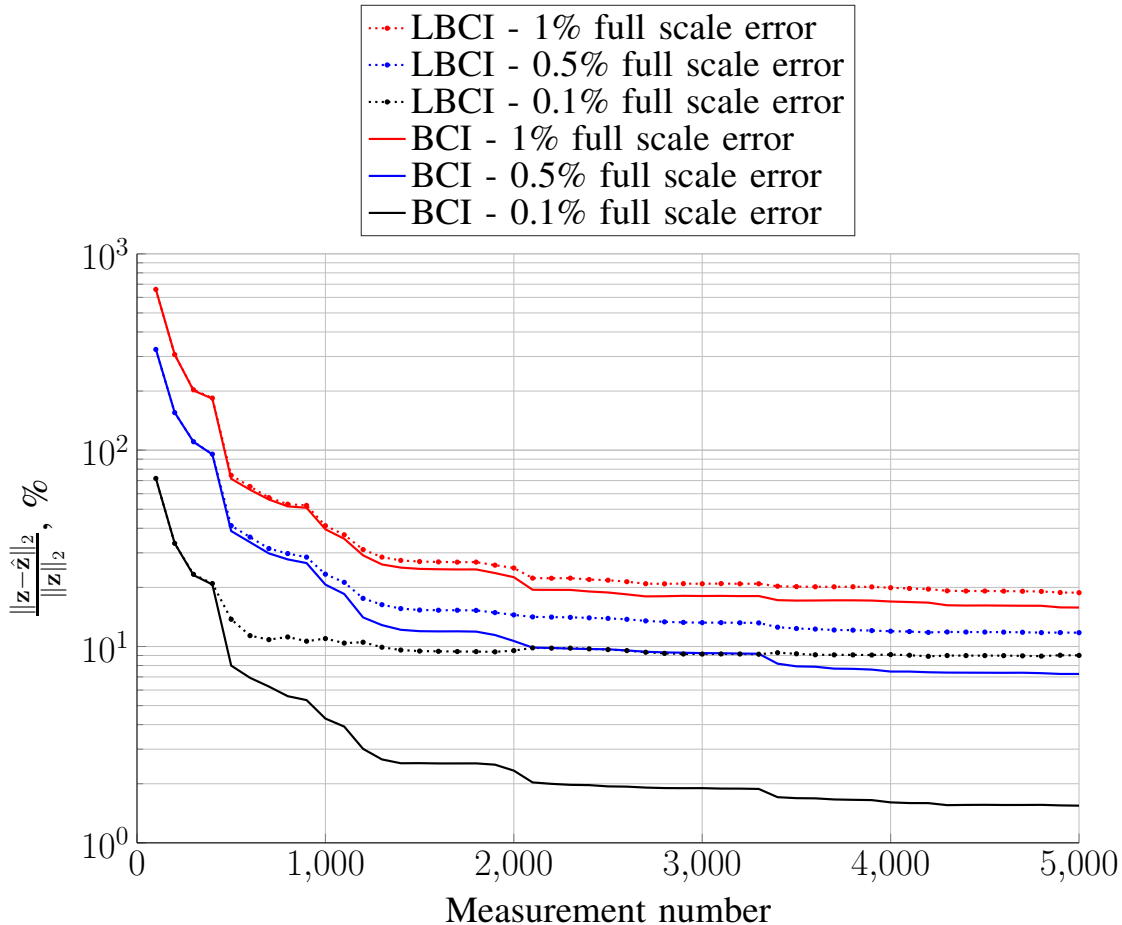


Fig. 9: Comparison of LBCI-old and BCI algorithms in the case of long power lines

It is noticeable how BCI outperforms LBCI-old by almost 50% in the case of 1% of the measurement error, by the factor of 2 when the error is 0.5% and by the factor of 10 when the measurements are very accurate (0.1%). Combining this with the previous results let us conclude that BCI algorithm (with regularisation in some cases) is recommended for usage instead of the conventional approach (LBCI-old).

## V. CONCLUSION

A novel power line impedance estimation method for the low-voltage grid has been proposed in this paper and a decentralised implementation suitable for smart meters has been developed. The BCI algorithm is iterative and based on least squares estimation making it very attractive for practical applications. We do not require phase synchronous measurements, and we propose modifications that take advantage of known  $X/R$  ratio to develop real-time distributed versions of our algorithms. Simulations in MATLAB have shown algorithm performance and key properties for different numbers of measurements and smart meters accuracy classes. We have also provided a theoretical framework that allows solution of a certain class of non-convex problems that can be generalised in future work. We will also address possible extensions of the BCI algorithm for topology identification and fault detection.

## VI. ACKNOWLEDGEMENTS

The authors would like to thank Steven Law and Iman Shames for useful comments and discussions.

## REFERENCES

- [1] Y.-F. Huang, S. Werner, J. Huang, N. Kashyap, and V. Gupta, "State estimation in electric power grids: Meeting new challenges presented by the requirements of the future grid," *IEEE Signal Processing Magazine*, vol. 29, no. 5, pp. 33–43, 2012.
- [2] D. Della Giustina, M. Pau, P. A. Pegoraro, F. Ponci, and S. Sulis, "Electrical distribution system state estimation: measurement issues and challenges," *IEEE Instrumentation & Measurement Magazine*, vol. 17, no. 6, pp. 36–42, 2014.
- [3] A. Y. Lam, B. Zhang, and N. T. David, "Distributed algorithms for optimal power flow problem," in *2012 IEEE 51st IEEE Conference on Decision and Control (CDC)*. IEEE, 2012, pp. 430–437.
- [4] A. Tarkiainen, R. Pollanen, M. Niemela, and J. Pyrhonen, "Identification of grid impedance for purposes of voltage feedback active filtering," *IEEE Power Electronics Letters*, vol. 2, no. 1, pp. 6–10, 2004.
- [5] A. J. Wood and B. F. Wollenberg, *Power generation, operation, and control*. John Wiley & Sons, 2012.
- [6] P. Jahangiri and D. C. Aliprantis, "Distributed volt/var control by pv inverters," *IEEE Transactions on power systems*, vol. 28, no. 3, pp. 3429–3439, 2013.
- [7] J. De La Ree, V. Centeno, J. S. Thorp, and A. G. Phadke, "Synchronized phasor measurement applications in power systems," *IEEE Transactions on Smart Grid*, vol. 1, no. 1, pp. 20–27, 2010.
- [8] J. Yang, W. Li, T. Chen, W. Xu, and M. Wu, "Online estimation and application of power grid impedance matrices based on synchronised phasor measurements," *IET generation, transmission & distribution*, vol. 4, no. 9, p. 1052, 2010.
- [9] G. Cavraro, R. Arghandeh, K. Poolla, and A. Von Meier, "Data-driven approach for distribution network topology detection," in *2015 IEEE Power & Energy Society General Meeting*. IEEE, 2015, pp. 1–5.
- [10] D. Deka, S. Backhaus, and M. Chertkov, "Estimating distribution grid topologies: A graphical learning based approach," in *Power Systems Computation Conference (PSCC), 2016*. IEEE, 2016, pp. 1–7.
- [11] D. Alahakoon and X. Yu, "Smart electricity meter data intelligence for future energy systems: A survey," *IEEE Transactions on Industrial Informatics*, vol. 12, no. 1, pp. 425–436, 2016.
- [12] S. Han, D. Kodaira, S. Han, B. Kwon, Y. Hasegawa, and H. Aki, "An automated impedance estimation method in low-voltage distribution network for coordinated voltage regulation," *IEEE Transactions on Smart Grid*, vol. 7, no. 2, pp. 1012–1020, 2016.
- [13] S. Cobreces, E. J. Bueno, D. Pizarro, F. J. Rodriguez, and F. Huerta, "Grid impedance monitoring system for distributed power generation electronic interfaces," *IEEE Transactions on Instrumentation and Measurement*, vol. 58, no. 9, pp. 3112–3121, 2009.
- [14] M. Ciobotaru, V. Agelidis, and R. Teodorescu, "Line impedance estimation using model based identification technique," in *Power Electronics and Applications (EPE 2011), Proceedings of the 2011-14th European Conference on*. IEEE, 2011, pp. 1–9.
- [15] M. Tariq and H. V. Poor, "Electricity theft detection and localization in grid-tied microgrids," *IEEE Transactions on Smart Grid*, 2016.
- [16] F. Van Der Bergh, P. Kadurek, S. Cobben, and W. Kling, "Electricity theft localization based on smart metering," in *21st International Conference on Electricity Distribution, Frankfurt, 2011*, pp. 1–4.
- [17] S. Sahoo, D. Nikovski, T. Muso, and K. Tsuru, "Electricity theft detection using smart meter data," in *Innovative Smart Grid Technologies Conference (ISGT), 2015 IEEE Power & Energy Society*. IEEE, 2015, pp. 1–5.
- [18] R. Diestel, "Graph theory, ser," *Graduate Texts in Mathematics*. Springer-Verlag, Heidelberg, vol. 173, 2005.
- [19] B. R. W. Group, "Smart metering infrastructure minimum functionality specification," , Tech. Rep., 2011. [Online]. Available: <https://link.aemo.com.au/sites/wcl/smartmetering/Pages/BRWG.aspx>
- [20] NMI, "M 6-1 electricity meters, part 1: Metrological and technical requirements," National Measurement Institute, Australia, Tech. Rep., 2012.
- [21] C. Brice, "Comparison of approximate and exact voltage drop calculations for distribution lines," *IEEE Transactions on Power Apparatus and Systems*, no. 11, pp. 4428–4431, 1982.
- [22] G. H. Golub, P. C. Hansen, and D. P. O'Leary, "Tikhonov regularization and total least squares," *SIAM Journal on Matrix Analysis and Applications*, vol. 21, no. 1, pp. 185–194, 1999.
- [23] J. Peppanen, M. J. Reno, R. J. Broderick, and S. Grijalva, "Distribution system secondary circuit parameter estimation for model calibration." Sandia National Lab.(SNL-NM), Albuquerque, NM (United States), Tech. Rep., 2015.

- [24] J. D. Glover, M. S. Sarma, and T. Overbye, *Power System Analysis & Design, SI Version, chapter 5*. Cengage Learning, 2012.
- [25] S. Barker, S. Kalra, D. Irwin, and P. Shenoy, "Empirical characterization and modeling of electrical loads in smart homes," in *Green Computing Conference (IGCC), 2013 International*. IEEE, 2013, pp. 1–10.
- [26] M. Pipattanasomporn, M. Kuzlu, S. Rahman, and Y. Teklu, "Load profiles of selected major household appliances and their demand response opportunities," *IEEE Transactions on Smart Grid*, vol. 5, no. 2, pp. 742–750, 2014.

## VII. APPENDICES

### APPENDIX

#### *Theoretical framework*

Consider the following optimisation problem:

$$\begin{aligned} \min_{\mathbf{x}, \mathbf{y}} \quad & f(\mathbf{x}, \mathbf{y}) \\ \text{subject to} \quad & \mathbf{y} = \mathbf{g}(\mathbf{x}). \end{aligned} \tag{16}$$

where:  $f(\mathbf{x}, \mathbf{y}) = \|\mathbf{Ax} - \mathbf{By} - \mathbf{c}\|_2^2$  with  $\mathbf{A} \in \mathbb{R}^{m \times n}$ ,  $\mathbf{B} \in \mathbb{R}^{m \times n}$ ,  $\mathbf{c} \in \mathbb{R}^m$  and  $\mathbf{g}(\mathbf{x})$  is a continuous and differentiable function. Introduce  $\mathbf{h}(\mathbf{y}) := \operatorname{argmin}_{\mathbf{x}} f(\mathbf{x}, \mathbf{y})$

**Lemma 1.** *Assume:*

- (1)  $\mathbf{A}$  and  $\mathbf{B}$  are full rank matrices;
- (2)  $\mathbf{g}: \mathbb{R}^m \rightarrow \mathbb{R}^m$  is surjective (onto) mapping;

Then  $\mathbf{y}^* = \mathbf{g} \circ \mathbf{h}(\mathbf{y}^*)$  and  $\mathbf{x}^* = \mathbf{h}(\mathbf{y}^*)$  give the solution  $(\mathbf{x}^*, \mathbf{y}^*)$  of the optimisation problem (16).

*Proof.*  $\mathbf{h}(\mathbf{y}) = \mathbf{A}^\dagger(\mathbf{By} + \mathbf{c})$  is a linear least squares solution. Provided that  $\mathbf{A}$  is a full rank matrix,  $\mathbf{h}(\mathbf{y})$  exists and unique for any  $\mathbf{y}$ . Thus  $\mathbf{h}(\mathbf{y})$  is an injective mapping.

Next, note that  $f(\mathbf{x}, \mathbf{y})$  is strictly convex. KKT conditions for (16) take the form:

$$\begin{aligned} \nabla_{\mathbf{x}} f(\mathbf{x}, \mathbf{y}) + \nabla_{\mathbf{y}} f(\mathbf{x}, \mathbf{y}) \nabla_{\mathbf{x}} \mathbf{g}(\mathbf{x}) &= 0, \\ \mathbf{y} &= \mathbf{g}(\mathbf{x}). \end{aligned} \tag{17}$$

Since  $\mathbf{B}$  is a full rank matrix,  $\nabla_{\mathbf{y}} f(\mathbf{x}, \mathbf{y}) \Big|_{\mathbf{x}=\mathbf{h}(\mathbf{y})} = \mathbf{0}$  and therefore  $\mathbf{h}(\mathbf{y})$  is a unique minimiser of  $f(\mathbf{x}, \mathbf{y})$ .

Observe that a solution of the problem (16) will necessarily satisfy:  $\begin{cases} \mathbf{x} = \mathbf{h}(\mathbf{y}), \\ \mathbf{y} = \mathbf{g}(\mathbf{x}), \end{cases}$  where from we conclude that the unique  $\mathbf{y}$  can be obtained if  $\mathbf{g} \circ \mathbf{h}$  form the inverse mapping, i.e.  $\mathbf{h}$  is the right inverse for  $\mathbf{g}$  and  $\mathbf{g}$  is the left inverse for  $\mathbf{h}$ . Therefore, using supplementary proposition that are given below:

- The function is injective if and only if it has a left inverse,
- The function is surjective if and only if it has a right inverse,

we prove the statement of the lemma. □

*Supplementary propositions*

**Proposition 7.** *Let  $X$  and  $Y$  are non-empty sets, then  $f: X \rightarrow Y$  is injective if and only if there exists  $g: Y \rightarrow X$  such that  $g \circ f = id_X$ .*

*Proof.* 1) Suppose there is  $g: Y \rightarrow X$  such that  $g \circ f = id_X$ . Let  $f(x) = f(y)$  then  $x = id_X(x) = g \circ f(x) = g \circ f(y) = id_X(y) = y$ , i.e.  $f(x) = f(y) \Rightarrow x = y$  which means that  $f: X \rightarrow Y$  is injective.

2) Suppose  $f: X \rightarrow Y$  is injective, i.e.  $f(x) = f(y) \Rightarrow x = y$ . Then if  $y \in \mathbf{im} f$ , there is unique  $x \in X: f(x) = y$ . Fix some  $x \in X$  and define  $g: Y \rightarrow X$  as follows:

$$g(y) = \begin{cases} f^{-1}(y), & \text{if } y \in \mathbf{im} f, \\ x, & \text{if } y \notin \mathbf{im} f, \end{cases}$$

Note that  $g \circ f(x) = f^{-1}(f(x)) = x$  by injectivity of  $f$  and construction of  $g$ . □

**Proposition 8.** *Let  $X$  and  $Y$  are non-empty sets, then  $f: X \rightarrow Y$  is surjective if and only if there exists  $g: Y \rightarrow X$  such that  $f \circ g = id_Y$ .*

*Proof.* 1) Suppose there is  $g: Y \rightarrow X$  such that  $f \circ g = id_Y$ . Then for each  $y \in Y$  there is  $x_y = g(y) \in X$  such that  $f \circ g(y) = f(x_y) = id_Y = y$ , i.e.  $f$  is surjective.

2) Suppose  $f: X \rightarrow Y$  is surjective. Then for all  $y \in Y$  there is  $x_y \in X$  such that  $f(x_y) = y$ . Define  $g: Y \rightarrow X$  so that it maps each  $y$  to  $x_y$ . Then  $\forall y \in Y: f \circ g(y) = f(x_y) = y$ , i.e.  $f \circ g = id_Y$ . □

*A. Proof of Proposition 6*

**Proposition.** *Let  $(z_n^{LBCI}, \mathbf{1})$  is the solution found by the LBCI algorithm and  $(z_n^{BCI}, \gamma_n^{BCI})$  is the solution found by the BCI algorithm. Also, let  $N(z_n, \gamma_n) := \|\mathbf{V}_{n-1}\gamma_n - \mathbf{v}_n - \mathbf{J}_n \mathbf{Q}_1 z_n\|_2^2 + \|\mathbf{V}_{n-1}\sqrt{\mathbf{1} - \gamma_n^2} - \mathbf{J}_n \mathbf{Q}_2 z_n\|_2^2$  then*

$$N(z_n^{BCI}, \gamma_n^{BCI}) \leq N(z_n^{LBCI}, \mathbf{1}),$$

*i.e. the BCI algorithm finds the solution that is closer to the optimum of (9) than that of LBCI.*

*Proof.* Consider a linearised BCI algorithm for the power line between nodes  $n - 1$  and  $n$ . The solution it finds satisfies:

$$\begin{aligned} N(z_n^{LBCI}, \mathbf{1}) &= \|\mathbf{V}_{n-1} - \mathbf{v}_n - \mathbf{J}_n \mathbf{Q}_1 z_n^{LBCI}\|_2^2 + \\ &+ \|\mathbf{J}_n \mathbf{Q}_2 z_n^{LBCI}\|_2^2 \geq \|\mathbf{V}_{n-1} - \mathbf{v}_n - \mathbf{J}_n \mathbf{Q}_1 z_n^{LBCI}\|_2^2. \end{aligned}$$

The corresponding expressions for  $z_n^{BCI}$  and  $z_n^{LBCI}$  are given by:

$$\begin{aligned} z_n^{BCI} &= [\mathbf{J}_n \mathbf{Q}_1]^\dagger (\mathbf{V}_{n-1} \gamma_n^{BCI} - \mathbf{v}_n), \\ z_n^{LBCI} &= [\mathbf{J}_n \mathbf{Q}_1]^\dagger (\mathbf{V}_{n-1} - \mathbf{v}_n), \end{aligned}$$

where  $\gamma_n^{BCI} \leq \mathbf{1}$ . Therefore:

$$\begin{aligned}
N(\mathbf{z}_n^{BCI}, \gamma_n^{BCI}) &= \|\mathbf{V}_{n-1}\gamma_n^{BCI} - \mathbf{v}_n - \mathbf{J}_n\mathbf{Q}_1\mathbf{z}_n^{BCI}\|_2^2 \leq \\
&\left\| [\mathbf{I} - \mathbf{J}_n\mathbf{Q}_1[\mathbf{J}_n\mathbf{Q}_1]^\dagger](\mathbf{V}_{n-1}\gamma_n^{BCI} - \mathbf{v}_n) \right\|_2^2 \leq \\
&\left\| [\mathbf{I} - \mathbf{J}_n\mathbf{Q}_1[\mathbf{J}_n\mathbf{Q}_1]^\dagger](\mathbf{V}_{n-1} - \mathbf{v}_n) \right\|_2^2 = \\
&\|\mathbf{V}_{n-1} - \mathbf{v}_n - \mathbf{J}_n\mathbf{Q}_1\mathbf{z}_n^{LBCI}\|_2^2 \leq N(\mathbf{z}_n^{LBCI}, \mathbf{1}).
\end{aligned}$$

□

*Corollary.* In the presence of high measurement noise, we can introduce a regularisation term (as in the LBCI case) for BCI algorithm so that:  $N(\mathbf{z}_n^{BCI}, \gamma_n^{BCI}) \leq N(\mathbf{z}_n^{LBCI}, \mathbf{1})$ .

*Proof.* To see this, note that:

$$\begin{aligned}
N(\mathbf{z}_n^{BCI}, \gamma_n^{BCI}) &\leq \left\| [\mathbf{I} - \mathbf{J}_n\mathbf{Q}_1[\mathbf{J}_n\mathbf{Q}_1]^\dagger](\mathbf{V}_{n-1} - \mathbf{v}_n) \right\|_2^2 \leq \\
&\left\| [\mathbf{I} - \mathbf{J}_n\mathbf{Q}_1[\mathbf{J}_n\mathbf{Q}_1]^\dagger](\mathbf{V}_{n-1} - \mathbf{v}_n) \right\|_2^2 + \mu \|\mathbf{J}_n\mathbf{Q}_2\mathbf{z}_n^{BCI}\|_2^2 \leq \\
&\left\| [\mathbf{I} - \mathbf{J}_n\mathbf{Q}_1[\mathbf{J}_n\mathbf{Q}_1]^\dagger](\mathbf{V}_{n-1} - \mathbf{v}_n) \right\|_2^2 + \|\mathbf{J}_n\mathbf{Q}_2\mathbf{z}_n^{LBCI}\|_2^2 = \\
&N(\mathbf{z}_n^{LBCI}, \mathbf{1}),
\end{aligned}$$

where  $0 \leq \mu \leq 1$  is a regularisation parameter.

□